Thermal proteome profiling monitors ligand interactions with cellular membrane proteins

Friedrich B M Reinhard[1,3], Dirk Eberhard[1,3], Thilo Werner[1], Holger Franken[1], Dorothee Childs[1,2], Carola Doce[1], Maria Fälth Savitski[1], Wolfgang Huber[2], Marcus Bantscheff[1], Mikhail M Savitski[1] & Gerard Drewes[1]

We extended thermal proteome profiling to detect transmembrane protein–small molecule interactions in cultured human cells. When we assessed the effects of detergents on ATP-binding profiles, we observed shifts in denaturation temperature for ATP-binding transmembrane proteins. We also observed cellular thermal shifts in pervanadate-induced T cell–receptor signaling, delineating the membrane target CD45 and components of the downstream pathway, and with drugs affecting the transmembrane transporters ATP1A1 and MDR1.

The recently developed cellular thermal-shift assay (CETSA) enables the monitoring of drug-target engagement, a key parameter in drug discovery, in live cells[1,2]. In the CETSA method, cell or cell extract samples are heated to different temperatures, allowing assessment of the effects of ligands on the thermal stability of a target protein. Most proteins unfold ('melt') and aggregate at defined temperatures, and subsequent analysis of the respective soluble fractions (e.g., by western blotting) results in a protein-aggregation curve, which is typically shifted by bound ligand[3–6].

The combination of the CETSA principle with quantitative proteomics[2,6] has enabled the thermal profiling of thousands of cellular proteins and extended the scope of the method for comprehensive assessment of the cellular proteins that interact with a ligand. This approach, termed thermal proteome profiling (TPP), was used to identify drug targets and off-targets potentially responsible for side effects and to determine target occupancy at different drug concentrations. Moreover, changes in thermal stability were also observed for downstream effectors of drug treatment, likely as a result of altered post-translational modifications[2]. However, CETSA- and TPP-based approaches have relied on the extraction of cells with a detergent-free buffer, and thus have been limited to ligand interactions with soluble, in most cases cytosolic, proteins. Because many ligand-binding receptors and drug targets are transmembrane proteins[7], this is a serious limitation of the method. After we submitted this paper for publication, a report was published that demonstrated a cellular thermal shift for the intracellular transmembrane protein STING binding to a nucleotide cofactor[8].

Here we extended the TPP approach to profile membrane-protein targets of small molecules. This method involved the use of a mild detergent during cell extraction (**Fig. 1a**). Our initial concern was that detergents might confound our results, for instance, by precluding heat-induced aggregation or by resolubilizing precipitated proteins. To test this, we heated K562 cells to 70 °C and then extracted them with SDS, Nonidet P-40 (NP-40), CHAPS, CHAPSO, DDM, β-octylglucoside, Brij 35 or Pluronic F127 and analyzed them by PAGE. Only SDS caused resolubilization of heat precipitates (**Supplementary Fig. 1**). We used NP-40 at a concentration of 0.4%, which proved sufficient to solubilize many membrane proteins but did not affect the determination of accurate protein-drug affinities in previous affinity proteomics studies[9,10].

In our first set of experiments we assessed the effects of NP-40 in the cell extract during the heating steps. As in our previous study[2], we investigated the thermal profiles of proteins annotated with the Gene Ontology (GO) term "ATP-binding" in K562 cell extracts with and without NP-40 (**Fig. 1a**). When we compared the melting (aggregation) temperatures of 2,196 proteins in detergent versus non-detergent experiments, we noted a clear trend of proteins aggregating at lower temperatures (2.9 °C lower on average (s.e.m. = 0.04); $P < 0.01$, t-test) in the presence of NP-40, indicating decreased thermal stability (**Fig. 1b** and **Supplementary Tables 1** and **2**). However, NP-40 did not substantially affect the shifts in protein melting temperatures (T_m) induced by the addition of physiological concentrations of MgATP to the cell extract, indicating that the interaction of proteins with ATP was not affected by the detergent (**Fig. 1c**).

As expected, membrane proteins were more abundantly identified in NP-40 extracts than in extracts without the detergent. We identified 371 membrane proteins with defined 'good-quality' melting curves (Online Methods and **Supplementary Tables 1** and **2**) in both biological replicates of the NP-40 experiment, compared with 75 membrane proteins with good-quality melting curves without NP-40 (possibly due to proteolysis or alternative splicing leading to loss of the transmembrane domain). A comparison of T_m density plots showed that membrane proteins tended to have lower thermal stability (average T_m of 47.2 °C, s.e.m. = 0.17) than non-membrane proteins (average T_m of 48.8 °C, s.e.m. = 0.06) (**Fig. 1d**). The detergent extract enabled the identification of ATP-binding membrane proteins on the basis of increased thermal stability in the presence of ATP, including the inner mitochondrial membrane proteins ABCB10 and BCS1L (**Fig. 1e**,**f**). NP-40 did not substantially affect the identification of nonmembrane ATP-binding proteins on the basis of ATP-induced thermal shifts (**Supplementary Table 3** and **Supplementary Fig. 2**). Thus, the method is in principle

[1]Cellzome GmbH, Molecular Discovery Research, GlaxoSmithKline, Heidelberg, Germany. [2]Genome Biology Unit, European Molecular Biology Laboratory, Heidelberg, Germany. [3]These authors contributed equally to this work. Correspondence should be addressed to M.M.S. (mikhail.m.savitski@gsk.com) or G.D. (gerard.c.drewes@gsk.com).

RECEIVED 3 JUNE; ACCEPTED 6 OCTOBER; PUBLISHED ONLINE 2 NOVEMBER 2015; DOI:10.1038/NMETH.3652

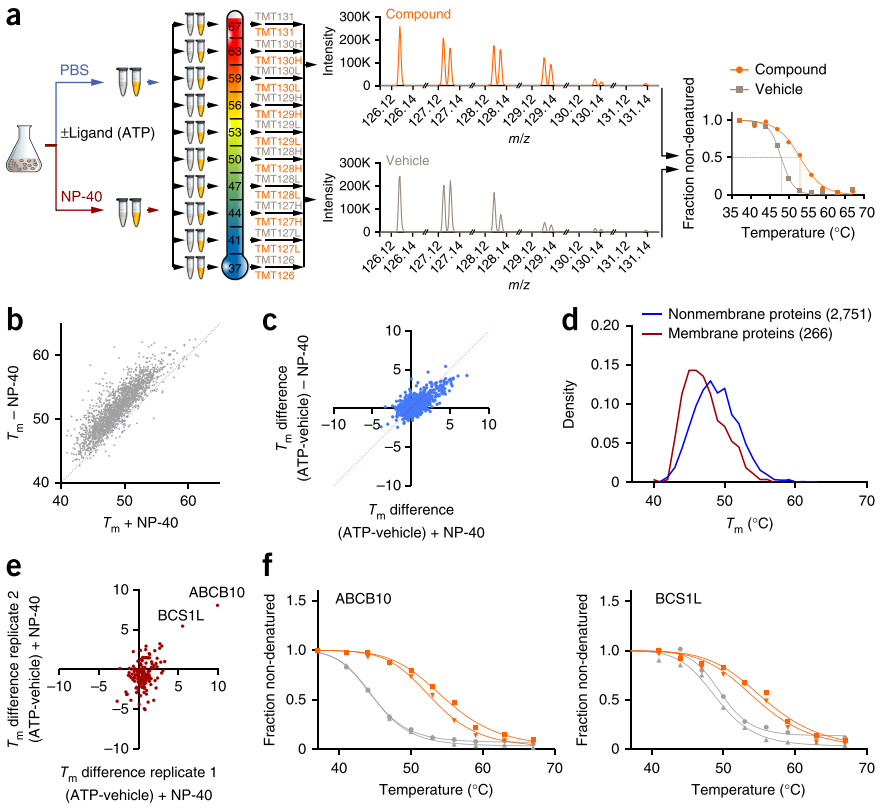

Figure 1 | TPP of ATP-binding proteins in cell extracts in the presence or absence of mild detergent. (**a**) Experiment outline. Cell extracts were generated using PBS with or without 0.4% NP-40, and aliquots were heated to different temperatures, digested, 10-plex tandem mass tag (TMT10) labeled and analyzed by mass spectrometry. Melting curves for vehicle-treated and ATP-treated cell extracts were fitted, and T_m shifts were inferred between the different treatment conditions. (**b**) Comparison of T_m values of 2,196 proteins in a K562 cell extract in the absence or presence of NP-40. Dashed line represents the identity line. (**c**) Comparison of T_m shifts induced by the addition of MgATP to cell extracts with or without NP-40. The minimum T_m shift for each protein was calculated from a pair of biological replicates. Dashed line represents the identity line. (**d**) Density plot of T_m values of membrane and nonmembrane proteins in NP-40 detergent extracts. (**e**) Comparison of T_m shifts for ATP-binding membrane proteins determined from two biological replicates. (**f**) Melting and aggregation curves for the inner mitochondrial membrane proteins ABCB10 and BCS1L in the presence (orange symbols) and absence (gray symbols) of ATP. Data from two independent replicate experiments are shown.

compatible with detergent extracts, but in some cases the type and concentration of detergent might need to be optimized for a given type of receptor or ligand class.

CETSA can also be performed with intact cells rather than cell extracts, and thereby provide target identification and target-occupancy information along with the identification of downstream effectors[1,2]. We investigated the T cell receptor (TCR) pathway, which can be stimulated by pervanadate in Jurkat lymphoma T cells[11] and has been extensively studied by proteomics[12]. Jurkat cells with or without stimulation by pervanadate were heated to different temperatures and then extracted in the presence or absence of NP-40 (**Fig. 2a** and **Supplementary Tables 4** and **5**). The presence of detergent during extraction after cell heating did not affect protein T_m values (**Fig. 2b**), in contrast to the presence of detergent in the cell extracts during heating described above (**Fig. 1b**). This further confirmed that the mild detergent did not resolubilize heat-precipitated proteins. A comparison of melting curves from both detergent and detergent-free settings did not indicate any substantial effects of detergent on the observed T_m shifts (**Fig. 2c** and **Supplementary Table 6**).

We identified 748 membrane proteins with good-quality melting curves (Online Methods) in both biological replicates in the detergent setting, as opposed to 77 in the detergent-free setting (**Supplementary Tables 4** and **5**). On average, membrane proteins in heated cells aggregated at higher temperatures (average T_m of 51.6 °C, s.e.m. = 0.13) (i.e., they had higher thermal stability) than nonmembrane proteins did (average T_m of 49.5 °C, s.e.m. = 0.06) (**Fig. 2d**). This contrasts with the lower thermal stability observed in heated cell extract (**Fig. 1d**), suggesting that the intact membrane environment provided a stabilizing effect. In the detergent-extracted cells, we reproducibly detected several membrane targets that showed thermal shifts after pervanadate treatment (**Fig. 2e**).

The primary target of pervanadate in the TCR pathway is the receptor tyrosine phosphatase CD45 (PTPRC)[11]. This transmembrane protein is irreversibly inhibited by pervanadate[13], and we observed destabilization in pervanadate-treated cells (**Fig. 2f**). Thermal destabilization has been reported previously for covalent inhibitors[14]. In addition, we found that the endoplasmic reticulum transmembrane protein SC4MOL was destabilized by pervanadate treatment. SC4MOL is genetically linked to insulin resistance and type 2 diabetes[15], and insulin signaling is known to be affected by pervanadate[16]. Two membrane proteins, desmoglein-2 and SLC12A9, showed robust stabilization after pervanadate treatment (**Fig. 2e** and **Supplementary Table 5**). Desmoglein-2 is described as a transmembrane glycoprotein present in desmosomes and was tyrosine-phosphorylated in response to pervanadate, leading to increased desmosome-mediated cell adhesion[17]. SLC12A9 is a predicted cation-chloride cotransporter of unknown physiological function. In addition to these transmembrane proteins, other components of the TCR pathway exhibited thermal shifts after pervanadate treatment (**Supplementary Fig. 3**), including multiple pathway components in the plasma membrane, such as CD45, LCK and FYN, and in the nucleus, such as JNK1 and NFAT (**Supplementary Fig. 4**). Besides the TCR pathway, several components of the 3-phosphoinositide degradation pathway also exhibited pervanadate-induced thermal shifts (**Supplementary Table 7**). There are no reported studies of this pathway with respect to pervanadate induction, but it is notable that most of the phospholipid-degradation reactions in the pathway are catalyzed by lipid phosphatases, which share a cysteine-dependent active site related to protein tyrosine phosphatases such as CD45 (ref. 18). Like CD45, several of these enzymes exhibited pervanadate-induced thermal destabilization, probably due to a similar oxidative inhibitory mechanism (**Supplementary Fig. 5**).

Finally, we tested our protocol with two chemical ligands for transporters that represent multipass transmembrane proteins for

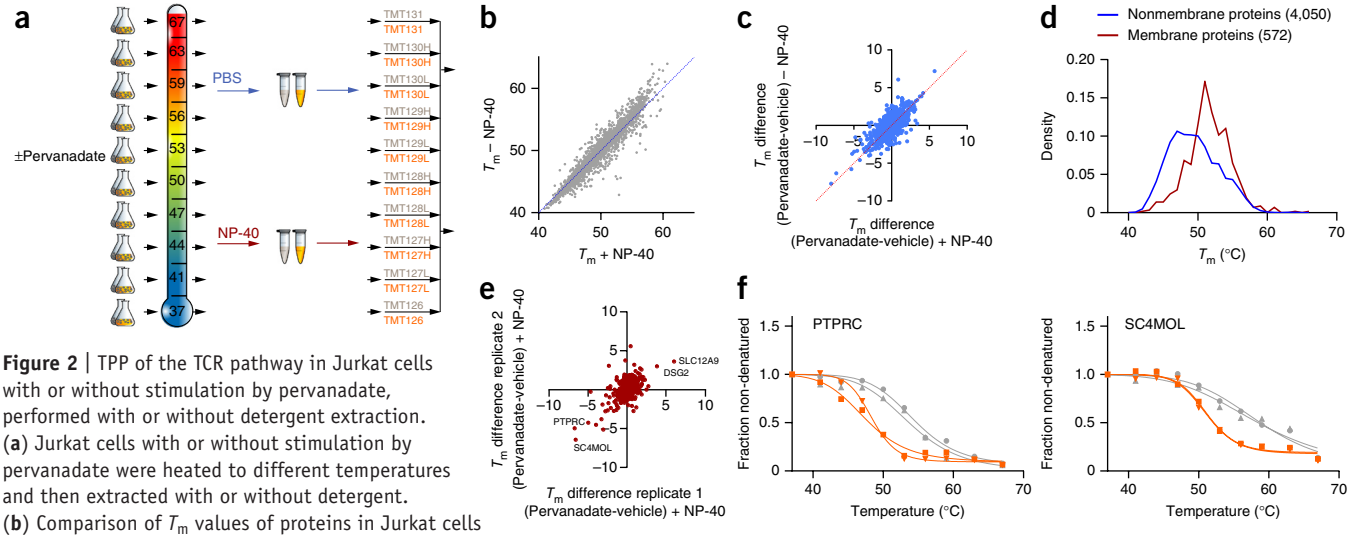

Figure 2 | TPP of the TCR pathway in Jurkat cells with or without stimulation by pervanadate, performed with or without detergent extraction. (**a**) Jurkat cells with or without stimulation by pervanadate were heated to different temperatures and then extracted with or without detergent. (**b**) Comparison of T_m values of proteins in Jurkat cells extracted with or without NP-40 after cell heating. Dashed line represents the identity line. (**c**) Comparison of T_m shifts induced by pervanadate treatment with subsequent generation of cell extracts with or without NP-40. The minimum T_m shift for each protein was calculated from a pair of biological replicate experiments. Dashed line represents the identity line. (**d**) Density plot of T_m values of membrane and nonmembrane proteins in intact cells. (**e**) Comparison of pervanadate-induced T_m shifts for membrane proteins determined from two biological replicates. (**f**) Melting and aggregation curves for the transmembrane proteins PTPRC (CD45) and SC4MOL in the presence (orange symbols) or absence (gray symbols) of pervanadate. Data from two independent replicate experiments are shown.

which it is typically difficult to assess ligand occupancy *in situ*. We assessed the effect of ouabain, a representative of a class of cardiotonic steroids used to treat hypotension and arrhythmia, on its target, the sodium-potassium ion pump[19]. Thermal profiling in K562 cells showed clear dose-dependent stabilization of two subunits of the pump, with half-maximal stabilization observed at low nanomolar concentrations of ouabain, demonstrating target occupancy at pharmacologically relevant concentrations (**Supplementary Table 8** and **Supplementary Fig. 6**). We also studied the effect of elacridar, a representative inhibitor of the multidrug-resistance transporter MDR1 (ref. 20), in adherent Caco-2 cells (**Supplementary Table 9** and **Supplementary Fig. 7**). We observed a T_m shift in MDR1 at pharmacologically relevant concentrations around 1 nM. In contrast to ouabain, elacridar elicited a destabilizing effect on its target, which may be explained by the fact that ABC transporters couple ATP binding and hydrolysis with substrate transport. Inhibitor binding may lead to the loss of ATP and its stabilizing effect on the transporter.

In summary, we have shown that the CETSA method, in particular in combination with quantitative proteomics, can be extended to transmembrane proteins, either in cell extracts or for *in situ* studies on intact cells. Membrane proteins on the cell surface and in intracellular organelles and vesicles undergo multiple interactions with drugs and with endogenous small-molecule ligands. Although challenges remain with respect to the identification of low-abundance targets and the robust detection of small temperature shifts, TPP provides a unique way to study drug-target engagement, to identify drug targets and off-targets, and to enable large-scale proteome-metabolite interaction studies.

METHODS

Methods and any associated references are available in the online version of the paper.

Accession codes. Mass spectrometry data are available for download at ProteomicsDB (accession PRDB004235).

Note: Any Supplementary Information and Source Data files are available in the online version of the paper.

ACKNOWLEDGMENTS

We thank J. Stuhlfauth for cell culture; M. Jundt, K. Kammerer, M. Klös-Hudak, M. Paulmann, I. Tögel and T. Rudi for expert technical assistance; and C.-W. Chung, J.W. Polli and M. Zamek-Gliszczynski for helpful suggestions.

AUTHOR CONTRIBUTIONS

F.B.M.R., M.M.S. and G.D. conceived the project; F.B.M.R., D.E., T.W., M.B., M.M.S. and G.D. designed the experiments; F.B.M.R., D.E. and T.W. conducted and supervised experiments; F.B.M.R., T.W., H.F., D.C., M.F.S., C.D., W.H., M.B., M.M.S. and G.D. contributed to data analysis; F.B.M.R. and M.B. contributed to the manuscript; and M.M.S. and G.D. wrote the manuscript.

COMPETING FINANCIAL INTERESTS

The authors declare competing financial interests: details are available in the online version of the paper.

1. Martinez Molina, D. *et al. Science* **341**, 84–87 (2013).
2. Savitski, M.M. *et al. Science* **346**, 1255784 (2014).
3. Huber, K.V. *et al. Nature* **508**, 222–227 (2014).
4. Jafari, R. *et al. Nat. Protoc.* **9**, 2100–2122 (2014).
5. Miettinen, T.P. & Bjorklund, M. *Mol. Pharm.* **11**, 4395–4404 (2014).
6. Franken, H. *et al. Nat. Protoc.* **10**, 1567–1593 (2015).
7. Overington, J.P., Al-Lazikani, B. & Hopkins, A.L. *Nat. Rev. Drug Discov.* **5**, 993–996 (2006).
8. Huber, K.V. *et al. Nat. Methods* doi:10.1038/nmeth.3590 (21 September 2015).
9. Bantscheff, M. *et al. Nat. Biotechnol.* **25**, 1035–1044 (2007).
10. Bantscheff, M. *et al. Nat. Biotechnol.* **29**, 255–265 (2011).
11. O'Shea, J.J., McVicar, D.W., Bailey, T.L., Burns, C. & Smyth, M.J. *Proc. Natl. Acad. Sci. USA* **89**, 10306–10310 (1992).
12. Matsumoto, M. *et al. Proteomics* **9**, 3549–3563 (2009).
13. Krejsa, C.M. *et al. J. Biol. Chem.* **272**, 11541–11549 (1997).
14. Dai, R., Wilson, D.J., Geders, T.W., Aldrich, C.C. & Finzel, B.C. *ChemBioChem* **15**, 575–586 (2014).
15. Chen, G. *et al. Hum. Mol. Genet.* **21**, 4530–4536 (2012).
16. Fantus, I.G., Kadota, S., Deragon, G., Foster, B. & Posner, B.I. *Biochemistry* **28**, 8864–8871 (1989).
17. Garrod, D.R., Fisher, C., Smith, A. & Nie, Z. *Cell Adhes. Migr.* **2**, 161–166 (2008).
18. Hsu, F. & Mao, Y. *Biochim. Biophys. Acta* **1851**, 698–710 (2015).
19. Laursen, M., Yatime, L., Nissen, P. & Fedosova, N.U. *Proc. Natl. Acad. Sci. USA* **110**, 10958–10963 (2013).
20. Wallstab, A., Koester, M., Bohme, M. & Keppler, D. *Br. J. Cancer* **79**, 1053–1060 (1999).

ONLINE METHODS

Reagents and cell culture. Reagents and media were purchased from Sigma-Aldrich unless otherwise noted. Ouabain was from Selleck, n-dodecyl-β-D-maltopyranoside was from Anatrace, and n-octyl-β-D-thioglucopyranoside and Brij 35 were from Thermo Fisher Scientific. The ATP1A1 antibody was from Santa Cruz (sc-28800), and the MDR1 antibody was from Abcam (ab168337). PBS was prepared using 137 mM NaCl, 2.7 mM KCl, 10 mM Na_2HPO_4 and 2 mM KH_2PO_4, pH 7.4, supplemented with one tablet of EDTA-free protease inhibitors (Roche Diagnostics) per 25 ml. K562, Jurkat E6.1 and Caco-2 cells were from ATCC. K562 cells were grown in RPMI medium containing 10% FCS at a maximum of 2×10^6 cells/ml, and Jurkat E6.1 cells were grown in RPMI 1640 medium supplemented with 4.5 g/l glucose, 10 mM HEPES, 1 mM sodium pyruvate and 10% FCS at a maximum of 10^7 cells/ml. Caco-2 cells were grown in MEM Earle's medium supplemented with 20% FCS. All cell lines were checked for mycoplasma contamination and authenticated using a Promega kit.

Preparation of K562 cell extract. K562 cultures (1.5×10^6 to 2×10^6 cells/ml) were centrifuged at 340*g* for 2 min at 4 °C and resuspended in 50 ml PBS. After a second wash step, the cells were resuspended in 10 ml of ice-cold PBS and centrifuged again at 340*g* for 2 min at 4 °C. Cells were resuspended in 1.5 ml of ice-cold PBS with or without 0.4% NP-40 (octylphenoxy poly(ethyleneoxy)ethanol). After resuspension, tubes were snap-frozen in liquid nitrogen, placed into a thermoshaker at 25 °C until ~60% of the content was thawed and then transferred onto ice until the entire content was thawed. This freeze-thaw cycle was repeated twice before ultracentrifugation (20 min at 4 °C and 100,000*g*). Protein concentration was determined by Bradford assay (Bio-Rad).

TPP of ATP in K562 cell extract. A solution of Mg-ATP in buffer[21] or buffer alone was added to the cell extract (the final MgATP concentration was 2 mM for PBS extract and 4 mM for detergent extract). The extract was incubated for 10 min at 25 °C, divided into ten aliquots of 100 µl and transferred into 0.2-ml PCR tubes. One each of the MgATP and the vehicle-containing samples was heated in parallel for 3 min to the appropriate temperature and then incubated for 3 min at room temperature. Subsequently the extract was centrifuged at 100,000*g* for 20 min at 4 °C. The supernatant was subjected to SDS gel electrophoresis and sample preparation for MS analysis[2].

TPP of pervanadate in Jurkat cells. Pervanadate was produced by mixing a 10 mM solution of sodium orthovanadate (Na_3VO_4) with a 110 mM H_2O_2 solution followed by incubation for 15 min at room temperature in the dark[11,22]. 72 µl of pervanadate solution was added to 24 ml of Jurkat cells (4×10^6 cells/ml) suspended in medium to yield a pervanadate concentration of 30 µM, after which cells were incubated for 30 min at 37 °C and 5% CO_2 and subsequently collected by centrifugation at 340*g* and 4 °C for 2 min. Cells were resuspended in 20 ml of ice-cold PBS and centrifuged again. This step was repeated once, and then the cells were resuspended in 1.2 ml of PBS. 100 µl of the suspension was transferred into 0.2-ml PCR tubes. After centrifugation at 325*g* for 2 min at 4 °C, 80 µl of the supernatant was removed. The cells were resuspended, and one each of the pervanadate and the vehicle-containing tubes was heated in parallel in a PCR block for 3 min to the reported temperature (37–67 °C) and then incubated for 3 min at room temperature. 30 µl of ice-cold PBS supplemented with 0.67% NP-40 and protease inhibitors was added to samples subjected to extraction in the presence of detergent; 30 µl of ice-cold PBS supplemented with EDTA-free protease-inhibitor cocktail was added to samples subjected to detergent-free extraction. Cells were snap-frozen in liquid nitrogen for 1 min, briefly thawed in a metal block at 25 °C, transferred onto ice and resuspended by pipetting. This freeze-thaw cycle was repeated once. The entire content was then centrifuged at 100,000*g* for 20 min at 4 °C. After centrifugation, 30 µl of the supernatant was transferred into a new tube. The supernatant was subjected to gel electrophoresis and sample preparation for MS analysis.

TPP of ouabain in K562 cells. 24 µl of 100% DMSO as vehicle or 1 mM ouabain dissolved in DMSO was added to 24 ml of suspension cells (1.4×10^6 cells/ml) in medium supplemented with 0.1% FCS and incubated for 60 min at 37 °C and 5% CO_2. Cell harvesting, heat treatment and cell lysis were done as described above. Soluble fractions were subjected to western blotting analysis using an ATP1A1 antibody. For isothermal dose-response experiments, ouabain was used in a seven-point serial dilution starting at 10 µM (concentrations were 10, 3.33, 1.11, 0.37, 0.12, 0.04 and 0.01 µM) including one vehicle control at 63 °C according to the procedure outlined above.

TPP of elacridar in Caco-2 cells. The medium of six confluent 15-cm dishes was exchanged for 20 ml of medium supplemented with 0.1% FCS, and 20 µl of vehicle (DMSO) or 20 µl of 1 mM elacridar was added to each of three dishes. Cells were incubated for 60 min at 37 °C and 5% CO_2. Subsequently, cells were washed with 20 ml of PBS before the addition of 3 ml of trypsin solution to each dish. After 10 min of incubation at 37 °C, 7 ml of PBS was added to each dish, and cells were transferred into Falcon tubes containing 35 ml of PBS and collected by centrifugation at 340*g* and 25 °C for 4 min. After resuspension in 8 ml of PBS, the three vehicle samples were combined in one Falcon tube, and the three elacridar samples were combined in another. Cells were harvested by centrifugation and washed once more with 20 ml of PBS. After sedimentation, cells were resuspended in 1.2 ml of PBS supplemented with protease inhibitors. Ten times 100 µl of each cell suspension was transferred into 0.2-ml PCR tubes. After centrifugation at 325*g* for 2 min at 25 °C, 80 µl of the PBS supernatant was removed. The cells were resuspended, and one each of the elacridar and vehicle samples was heated in a PCR machine for 3 min to the reported temperatures (37–67 °C) and then incubated for 3 min at room temperature. 30 µl of ice-cold PBS supplemented with 1.34% NP-40 was added to each tube. Subsequently, samples were subjected to two freeze-thaw cycles. Soluble fractions were subjected to western blotting analysis using an MDR1 antibody. For ITDR experiments, a four-point serial dilution of elacridar starting at 0.5 µM (concentrations were 0.5, 0.1, 0.02 and 0.0008 µM) was prepared and used for cell treatment including one vehicle control. For each condition, one 15-cm dish with Caco-2 cells was used. After treatment, cells were washed, harvested by the addition of trypsin and resuspended in 650 µl of PBS supplemented with protease inhibitors. 100 µl of the cell suspension was subjected to 3 min of heat treatment at fixed

doi:10.1038/nmeth.3652

temperatures of 54 °C and 56 °C as described above. Soluble fractions were subjected to gel electrophoresis and sample preparation for MS analysis. The five samples obtained by heating to 54 °C and the five samples obtained by heating to 56 °C were combined in one TMT10 experiment.

MS sample preparation and LC-MS/MS analysis. Gel lanes were cut into three slices covering the entire separation range (~2 cm) and subjected to in-gel digestion either with LysC (Wako Chemicals) for 2 h followed by trypsin (Promega) overnight or with trypsin only for 4 h (refs. 9,10). Peptide samples were labeled with TMT10 (Thermo Fisher Scientific) reagents. The labeling reaction was performed in 40 mM triethylammoniumbicarbonate, pH 8.53, at 22 °C and quenched with glycine. Labeled peptide extracts were combined into a single sample per experiment and subjected to additional fractionation on an Ultimate3000 (Dionex) by reversed-phase chromatography at pH 12 on a 1-mm Xbridge column (Waters), and 24 or 34 fractions were collected[23]. Depending on the analytical depth required, 8–17 fractions were analyzed by LC-MS. Samples were vacuum-dried and resuspended in 0.05% trifluoroacetic acid. 50% of the sample was injected into an Ultimate3000 nanoRLSC (Dionex) coupled to a Q Exactive Orbitrap mass spectrometer operated with Tune 2.3 and Xcalibur 3.0.63 (Thermo Fisher Scientific). Peptides were trapped on a 5 mm × 300 µm C18 column (Pepmap100, 5 µm, 300 Å, Thermo Fisher Scientific) in 0.05% TFA at 60 °C. Separation was performed on custom 50 cm × 100 µM (inner diameter) reversed-phase columns (Reprosil) at 55 °C. Gradient elution was performed from 2% acetonitrile to 40% acetonitrile in 0.1% formic acid and 3.5% DMSO over 2 h. Mass spectrometers were operated with online injection and a data-dependent top-ten acquisition protocol[24] using 70,000 resolution and an ion target set to 3×10^6. Higher energy collision dissociation (HCD) scans were performed with 35% normalized collision energy at 35,000 resolution at m/z 200 with an ion target setting of 2×10^5 to avoid coalescence.

Peptide and protein identification and quantification. Mascot 2.4 (Matrix Science) was used for protein identification; we selected a 10-ppm mass tolerance for peptide precursors and 20-mDa (HCD) mass tolerance for fragment ions. Carbamidomethylation of cysteine residues and TMT modification of lysine residues were selected as fixed modifications; methionine oxidation, N-terminal acetylation of proteins and TMT modification of peptide N termini were selected as variable modifications. The search database consisted of a customized version of the IPI database combined with a decoy version of the database created using a script supplied by Matrix Science (http://www.matrixscience.com/help/decoy_help.html). The following criteria were used for protein identifications: (i) For single spectrum to sequence assignments, we required that the assignment be the best match and have a minimum Mascot score of 31 and that there be a 10× difference between the assignment and the next best assignment. On the basis of these criteria, the decoy search results indicated <1% false discovery rate. (ii) For multiple spectrum to sequence assignments, using the same parameters, the decoy search results indicated <0.1% false discovery rate. Reporter ion intensities were extracted from the raw data and multiplied with ion accumulation times (in milliseconds) to yield a measure proportional to the number of ions; this measure is referred to as the ion area[25]. Peptide-spectrum matches were filtered according to the following criteria: Mascot ion score of >15, signal-to-background value of the precursor ion of >4 and signal-to-interference value of >0.5 (ref. 26). Fold changes were corrected for isotope purity as previously described and adjusted for interference caused by coeluting nearly isobaric peaks as estimated by the signal-to-interference measure[27]. Protein quantification values were calculated from individual spectra matching to unique peptides using a sum-based bootstrap algorithm; 95% confidence intervals were calculated for all protein fold changes that were quantified with more than three spectra[25]. We used the UniProt transmembrane domain annotation to classify proteins as membrane proteins by mapping the UniProt I.D.s on the IPI I.D.s.

Data analysis. After normalization, melting curves were fitted with the following equation as previously described[2], computed in R:

$$f(T) = \frac{1 - \text{plateau}}{1 + e^{-\left(\frac{a}{T} - b\right)}} + \text{plateau}$$

where T is the temperature and a, b and "plateau" are constants. The value of $f(T)$ at the lowest temperature T_{min} was fixed to 1. The melting point of a protein is defined as the temperature T_{m} at which half of the protein amount has been denatured, i.e.,

$$f(T_{\text{m}}) = 0.5$$

for proteins whose curves met the following three requirements: (i) fitted curves for both vehicle and compound-treated conditions had an R^2 of >0.8, (ii) the vehicle curve had a plateau of <0.3 and (iii) in each biological replicate the steepest slope of the protein melting curve in the paired set of vehicle and compound-treated conditions was below −0.06. In the visualization of data in **Figures 1c**,**e** and **2c**,**e**, we additionally required that the melting points measured in both vehicle replicates differ by <1.5 °C for the same protein. As in our previous study[2], given the stringent requirements on the quality of the curve fits of the compared proteins, we allowed proteins quantified with single peptides to be part of the analysis. In order to select proteins with significantly changed thermal stability after treatment in two biological replicates (two pairs of vehicle and compound-treated experiments), we used the following rules as previously described[2]:

- The melting point difference between vehicle and compound-treated conditions for a protein had a Benjamini-Hochberg–corrected P value (calculated as described[2]) of <0.05 in one biological replicate and <0.10 in the other.
- Both melting point differences were either positive or negative in the two biological replicates.
- The smallest absolute melting point difference of the protein in the two biological replicates was greater than the absolute melting point difference of that same protein between the two vehicle experiments.

Calculation of pEC_{50} values from thermal-profiling experiments over a compound concentration range. Vehicle conditions were used as the reference for fold-change calculations. Before fitting

of a sigmoidal dose-response curve (top and bottom fixed at 1 and 0; variable slope), all fold-change values were transformed so that they would range between 0 and 1 for stabilized proteins and between 1 and 0 for destabilized proteins[2,6]. We required proteins to be stabilized or destabilized by the compound treatment at the maximum concentration by at least 50% (untransformed fold changes) compared to the vehicle condition, and the R^2 of the fit of the sigmoidal dose-response curve had to be >0.8 (refs. 2,6). These conditions had to be fulfilled in both biological replicates. Proteins had to be identified by at least two unique peptides in both experiments. Proteins meeting these requirements were considered as affected in their thermal stability in a dose-response manner with the calculated pEC_{50} values.

Pathway analysis and visualization. Pathway analysis was performed with Ingenuity software (Qiagen). Of the 4,281 proteins (melting curves meeting the quality criteria described above[2] and with less than a 1.5 °C difference in melting point between vehicles) that were uploaded, 4,176 could be mapped in Ingenuity using the IPI accessions as identifiers. To assess affected pathways, we performed a core analysis calling proteins with an absolute temperature shift of at least 1.5 °C as significant and using the full uploaded data set as background. In addition, the following settings were used: data sources, all; confidence, experimentally observed; species, human; tissues and cell lines, all; and mutations, all. Membrane protein topologies were depicted using Protter[28].

21. Becher, I. *et al. ACS Chem. Biol.* **8**, 599–607 (2013).
22. Stoevesandt, O. *et al. Mol. Cell. Proteomics* **6**, 503–513 (2007).
23. Kruse, U. *et al. Leukemia* **25**, 89–100 (2011).
24. Werner, T. *et al. Anal. Chem.* **86**, 3594–3601 (2014).
25. Savitski, M.M. *et al. Anal. Chem.* **83**, 8959–8967 (2011).
26. Savitski, M.M. *et al. J. Am. Soc. Mass Spectrom.* **21**, 1668–1679 (2010).
27. Savitski, M.M. *et al. J. Proteome Res.* **12**, 3586–3598 (2013).
28. Omasits, U., Ahrens, C.H., Muller, S. & Wollscheid, B. *Bioinformatics* **30**, 884–886 (2014).

doi:10.1038/nmeth.3652